

---

# DIAGNOSTICS FOR INDIVIDUAL-LEVEL PREDICTION INSTABILITY IN MACHINE LEARNING FOR HEALTHCARE

---

**Elizabeth W. Miller**  
School of Data Science  
University of Virginia  
Charlottesville  
zrc3hc@virginia.edu

**Jeffrey D. Blume**  
School of Data Science  
University of Virginia  
Charlottesville  
blume@virginia.edu

## ABSTRACT

In healthcare, predictive models increasingly inform patient-level decisions, yet little attention is paid to the variability in individual risk estimates and its impact on treatment decisions. For overparameterized models, now standard in machine learning, a substantial source of variability often goes undetected, creating an illusion of reliability. Even when the data and model architecture are held fixed, randomness introduced by optimization and initialization can lead to materially different risk estimates for the same patient. This problem is largely obscured by standard evaluation practices, which rely on aggregate performance metrics (e.g., AUC-ROC, log-loss) that are agnostic to individual-level reliability. As a result, models with indistinguishable aggregate performance can nonetheless exhibit substantial procedural arbitrariness, undermining clinical trust and decision consistency. To diagnose the problem, we propose an evaluation framework that quantifies individual-level prediction instability across repeated instantiations of an otherwise fixed learning pipeline. The framework introduces two complementary diagnostics: empirical prediction interval width (ePIW), which captures variability in continuous risk estimates, and empirical decision flip rate (eDFR), which measures instability in threshold-based clinical decisions. We apply these diagnostics to simulated data and 30-day mortality following myocardial infarction (GUSTO-I) dataset [1]. Across settings, we find that for overparameterized machine-learning models, randomness arising solely from optimization and initialization can induce individual-level variability comparable to that produced by resampling the entire training dataset. Although logistic regression and neural networks often achieve similar aggregate performance, neural networks exhibit substantially greater instability in individual risk predictions, particularly near clinically relevant decision thresholds where small perturbations can alter treatment recommendations. These findings indicate that standard evaluation practices are insufficient for assessing clinical reliability and that stability diagnostics should be incorporated into routine model validation; when predictive accuracy is comparable, individual-level reliability should be a primary criterion for model selection.

**Keywords** individual-level prediction stability · prediction uncertainty · algorithmic randomness

## 1 Introduction

Machine learning (ML) is frequently positioned as the next frontier for clinical support [2]. ML models have shown promise in selected applications, such as clinical documentation and operational workflows. Yet the adaptation of clinical risk stratification models remains stubbornly low [3]. In a recent commentary, *All models are wrong and yours are useless: making clinical prediction models impactful for patients*, Markowitz highlights the systemic disconnect between controlled experimental success and clinical deployment, noting that clinicians' ethical and professional responsibilities to patients impose far stricter standards than those typically reflected in academic evaluation [4]. Fulfilling these responsibilities requires a degree of model reliability that is often undermined by a specific, invisible driver: individual-level prediction instability. We demonstrate that for overparameterized and flexible machine learning

models, a patient’s risk estimate and the resulting clinical decision can hinge on the arbitrary randomness of the learning pipeline.

While prior research has explored how data sampling or feature selection introduces uncertainty in the individual predictions [5, 6], standard evaluation practices largely ignore evaluating the stochasticity inherent in the optimization process itself. For overparameterized models, which now dominate machine learning research, we find that retraining a model, while holding many elements of the learning pipeline fixed (e.g., data, architecture, and hyperparameters), can produce materially different clinical recommendations for the same individual based solely on changes in the random seed initialization. This creates an inherent unreliability; a model may boast high aggregate accuracy, yet its specific predictions for high-stakes patients remain fundamentally unstable.

Standard aggregate metrics (e.g., AUC-ROC, log-loss, accuracy) are agnostic to this individual-level volatility. They average away the very instability that undermines clinician trust. There has been limited systematic study of how models with differing expressive capacity and optimization procedures exhibit behavioral differences in the prediction space, and how these differences could influence model selection in clinical risk settings. Although variability induced by resampling the training data is often viewed as the dominant source of predictive uncertainty, we find that randomness arising purely from optimization and weight initialization can induce divergent predictive behaviors across different trained fits, even when task-level performance is comparable. If two models achieve identical aggregate performance, but one flips a patient’s treatment recommendation 20% of the time based on a random initialization, that model is less reliable for clinical use. Yet, under current validation paradigms, these models can be treated as equivalent.

To address these challenges, we propose a general evaluation framework to quantify individual-level stability across repeated instantiations of the learning pipeline. Applying this framework to controlled simulations and the GUSTO-I clinical dataset [1], we compare models of differing expressive capacity under matched task-level performance. Our experiments reveal that models with stronger structural assumptions, such as logistic regression, consistently exhibit greater stability than flexible neural networks, which remain highly sensitive to algorithmic randomness.

These findings provide the basis for the following primary contributions:

1. We demonstrate the disconnect between aggregate performance and individual-level procedural consistency, where a model can exhibit stable out-of-sample performance yet exhibit unstable individual-level predictions.
2. We propose a framework to operationalize instability through two complementary diagnostics: empirical prediction interval width (ePIW), which measures the dispersion of continuous risk estimates, and empirical decision flip rate (eDFR), which captures the frequency of inconsistent binary clinical actions. This framework treats algorithmic randomness as a source of predictive uncertainty.
3. Using both synthetic experiments and clinical data (GUSTO-I), we reveal how instability is distributed across patient populations. We show that instability can occur near or away from decision boundaries. This introduces a vital nuance, such that even when a risk estimate does not trigger a ‘decision flip’, higher instability in the underlying estimate can undermine clinician trust in the model’s precision.
4. We translate these technical insights into a selection criterion for high-stakes healthcare. We argue that when predictive accuracy is comparable, more constrained model classes can offer greater reliability without sacrificing task-level performance.

## 2 Background and Related Work

For any given clinical prediction task, there often exists a vast set of models that achieve nearly indistinguishable out-of-sample performance. This collection, known as the *Rashomon set*, comprises models that may yield near-identical aggregate scores, such as Mean Squared Error (MSE) or AUC-ROC, while relying on fundamentally different decision logic [7, 8]. The transition toward overparameterized models, where the parameter count ( $p$ ) exceeds the training sample size ( $n$ ), has exponentially expanded this space of competitive but divergent solutions [9, 10].

This multiplicity is frequently framed as a problem of *underspecification*: standard training objectives are often too coarse to uniquely define a model’s behavior [11]. Consequently, models that appear equivalent based on aggregate metrics may exhibit meaningfully conflicting predictions for the same individual upon retraining [12, 13]. In a clinical context, this suggests that the “best” model may be selected based on arbitrary stochastic factors rather than superior medical insight or biological truth.

Healthcare literature has recognized the risk involved when machine learning (ML) models are sensitive to pipeline design, including in the context of variable selection [5] and individual-level risk predictions [6, 14]. However, this analysis has primarily focused on the underparameterized regime ( $p < n$ ). In contrast, modern flexible models rely on stochastic optimization procedures that are essential for convergence but induce divergent behaviors across fits [12, 15].

Recent evidence suggests that initialization and training dynamics alone can lead to significant predictive variance, even when task-level performance is matched [16, 17]. Furthermore, apparent differences in method performance can be driven as much by choices in the benchmarking protocol as by the modeling approach itself [18].

Statistical perspectives of this instability, which often analyzes the stability of predictions purely as a function of the data, can be disjointed from modern practice because statistical perspective treat optimization as a singular path to a global optimum. In the overparameterized and flexible models (e.g., neural networks), the "optimal" solution is not a single coordinate but one of many equally performing points scattered across a complex and sometimes non-convex loss landscape [19]. By ignoring the stochastic nature of how we navigate this landscape, current validation paradigms fail to account for the instability inherent across the entire learning pipeline. We aim to fill this gap by examining how model capacity acts as a catalyst for procedural instability, making individual risk estimates a function of the optimization process rather than the patient’s data.

### 3 Stability Metrics and Evaluation Framework

We consider the standard supervised learning setting where observations  $(X, Y)$  are drawn from an unknown joint distribution, yielding a dataset  $D = \{(x_i, y_i)\}_{i=1}^n$ . A standard training–evaluation paradigm partitions  $D$  into a training set  $D_{\text{train}}$  and a test set  $D_{\text{test}}$ . A fitted predictor  $\hat{f}$  is obtained by applying a learning pipeline  $\mathcal{A}$  to the training data. Modern learning pipelines often involve stochastic optimization, non-convex objectives, or both. To make this explicit, we write the fitted model from the  $b$ –th run as

$$\hat{f}^{(b)} = \mathcal{A}(D_{\text{train}}^{(b)}, f, \phi, \gamma),$$

where  $D_{\text{train}}^{(b)}$  denotes a (possibly perturbed) version of the training data,  $f \in \mathcal{H}$  denotes a model specification within hypothesis space  $\mathcal{H}$ ,  $\phi$  is a fixed loss function,  $\gamma$  denotes hyperparameter settings. Hyperparameter settings control both fixed (e.g., learning rate) and random (e.g., weight initialization) aspects of the learning pipeline.

Model architectures that are convex (e.g., linear models, logistic regression) tend to produce singular solutions if optimized using standard solvers (e.g., L-BFGS in scikit-learn) under a fixed dataset. Conversely, model architectures that are non-convex or overparameterized (e.g., overparameterized neural networks, random forest) can produce many plausible fitted solutions. Depending on the complexity of the data and the hypothesis space, different model architectures can produce similar out-of-sample performance. We formalize this collection of models as the set of competitive predictors. Let  $\hat{L}_{\text{test}}(f)$  denote the empirical test loss under  $\phi$ . For a tolerance  $\varepsilon \geq 0$ , we define the competitive set as:

$$\hat{\mathcal{R}}_{\text{set}}(\mathcal{H}, \varepsilon) = \left\{ f \in \mathcal{H} : \hat{L}_{\text{test}}(f) \leq \min_{g \in \mathcal{H}} \hat{L}_{\text{test}}(g) + \varepsilon \right\}.$$

This set represents a region of empirical indistinguishability in function space such that predictors within  $\hat{\mathcal{R}}_{\text{set}}$  are equivalent up to tolerance  $\varepsilon$  with respect to aggregate test performance [8]. In our experiments,  $\phi$  is the binary cross-entropy (BCE) loss, and  $\mathcal{H}$  is defined by the model specifications described in Section 3.3.

#### 3.1 Individual-Level Evaluation Metrics

While the competitiveness criterion ensures stability in the aggregate performance metrics, it does not guarantee consistency in the specific risk estimates  $\hat{f}(x_i)$  assigned to individual observations. We analyze the resulting instability as arising from two distinct pathways within the learning pipeline: (1) perturbations to the training data  $D_{\text{train}}$  and (2) stochasticity inherent in the optimization routine.

We represent the collection of predictions assigned to a specific individual across  $B$  repeated instantiations of the learning pipeline  $\mathcal{A}$  as:

$$\hat{P}_i := \{\hat{f}^{(b)}(x_i)\}_{b=1}^B,$$

where each  $\hat{f}^{(b)}$  satisfies the competitiveness criterion. Here,  $\hat{P}_i$  is a vector of  $B$  scalar predictions corresponding to individual  $x_i$ . Collectively, the predictions for all  $n$  test individuals across  $B$  competitive runs form an  $n \times B$  prediction matrix,  $\hat{\mathbf{P}}$ . If the dispersion for each row in  $\hat{\mathbf{P}}$  is large, then the pipeline is individually unstable for that observation, even if the models are globally equivalent. We quantify this dispersion using both continuous and categorical stability metrics introduced below.

### 3.1.1 Empirical Prediction Interval Width (ePIW)

For each individual  $x_i$ , let  $\widehat{P}_i$  denote the  $B \times 1$  vector of predicted risks obtained across repeated instantiations of the learning pipeline. We seek to quantify the effective support of the central distribution of this prediction set, i.e., the range of risk values that may plausibly be assigned to a given individual under learning pipeline variability.

For a nominal coverage level  $1 - \alpha$ , let  $Q_{\alpha/2}(\widehat{P}_i)$  and  $Q_{1-\alpha/2}(\widehat{P}_i)$  denote the lower and upper empirical quantiles of prediction set  $\widehat{P}_i$ . We define the empirical prediction interval width (ePIW) for individual  $x_i$  as

$$\text{ePIW}(x_i, \alpha) = Q_{1-\alpha/2}(\widehat{P}_i) - Q_{\alpha/2}(\widehat{P}_i).$$

In our experiments, we use  $\alpha = 0.05$ , corresponding to the central 95% of the empirical prediction distribution. Larger values of ePIW indicate greater dispersion in the prediction space for a given individual. Conversely,  $\text{ePIW} = 0$  implies that the predicted risk is invariant across all applied realizations of the learning pipeline and is therefore deterministic relative to the chosen model class and training procedure. Conceptually, ePIW answers the question: *What is the range of plausible risk scores an individual might receive from models with comparable aggregate performance?*

### 3.1.2 Empirical Decision Flip Rate (eDFR)

While ePIW captures dispersion in continuous risk estimates, many practical applications of machine learning rely on thresholded binary decisions. To assess the stability of such decisions, let  $\tau \in (0, 1)$  denote a fixed decision threshold. For each learning pipeline instance  $b$ , we define the induced binary decision for individual  $x_i$  as:

$$\hat{d}_i^{(b)}(\tau) = \mathbb{I}\{\hat{f}^{(b)}(x_i) \geq \tau\},$$

where  $\mathbb{I}\{\cdot\}$  denotes the indicator function.

We define the empirical decision flip rate (eDFR) for individual  $x_i$  as the proportion of distinct pairs of pipeline instantiations that disagree in their induced binary decision:

$$\text{eDFR}(x_i, \tau) = \frac{2}{B(B-1)} \sum_{1 \leq b < b' \leq B} \mathbb{I}\{\hat{d}_i^{(b)}(\tau) \neq \hat{d}_i^{(b')}(\tau)\}.$$

The eDFR takes values in  $[0, 1]$ , where values near 0 indicate highly stable binary decisions. Conceptually, eDFR answers the question: *How often does an individual's classification change when the model is refit?* This metric is particularly salient for clinical decision-making, as excessive classification flipping across competitive models undermines the perceived reliability and trustworthiness of algorithmic recommendations.

## 3.2 Model Classes Considered

We consider candidate predictors drawn from two broad model families: logistic regression and feedforward neural networks. These classes were selected to span a range of expressive capacity, from constrained parametric specifications to flexible, overparameterized architectures. The specific architectural choices are not the primary focus of this study; rather, these models serve as representative instances within a competitive set of predictors that achieve comparable aggregate out-of-sample performance.

All models considered produce predicted risks in the unit interval and are trained using binary cross-entropy (BCE) loss with  $L_2$  regularization to prevent overfitting and ensure numerical stability. Model configurations are selected to satisfy the competitiveness criterion defined above. Table 1 summarizes the model specifications and fitting routines used in our simulation and clinical risk prediction experiments.

Table 1: Model specifications for candidate architectures used in simulation and GUSTO-I experiments. The parameter count  $p$  reflects the total number of trainable weights and biases.

Abbreviation	Model Family	Specification & Fitting Routine	$p$
Log-LBFGS	Logistic Regression	Quasi-Newton (L-BFGS), $L_2$ reg.	6
Log-G	Logistic Regression	Quasi-Newton (L-BFGS), $L_2$ reg.	9
Log-SGD	Logistic Regression	SGD, $L_2$ reg.	6
Log-Poly	Logistic Regression	L-BFGS, $L_2$ reg., polynomial features	21
NN-1L	Neural Network	1 hidden layer (width 40), ReLU, SGD	281
NN-2L	Neural Network	2 hidden layers (width 180), ReLU, SGD	33,841
NN-G	Neural Network	2 hidden layers (width 180), ReLU, SGD	34,381

## 4 Experiments and Results

### 4.1 Experimental Design

We evaluate individual-level prediction stability under two distinct sources of learning-pipeline variability: (i) variation in the training data and (ii) stochasticity in the optimization procedure. To isolate data-driven instability, we employ a subsampling approach. For the simulated experiments, training sets are drawn directly from the known data-generating population. For the clinical experiments, training sets of size  $n_{\text{train}}$  are sampled without replacement from the larger GUSTO-I dataset.

Across all experiments, each model specification is retrained  $B = 100$  times and evaluated on a respective fixed test set of size  $n_{\text{test}} = 10,000$ . For the simulation, this test set was drawn from the population distribution, while for the clinical experiments, it is a held-out portion of the GUSTO-I dataset. This fixed set serves as a proxy for a stable deployment population, allowing us to measure how individual risk estimates fluctuate across refits. We consider two training sample sizes,  $n_{\text{train}} \in \{500, 5000\}$ , to examine how instability evolves with increased data availability.

For optimization-driven variability, the training data remains fixed while random seeds are varied to control weight initialization and the sequence of mini-batch updates in stochastic gradient descent. All models are trained using binary cross-entropy (BCE) loss with  $L_2$  regularization. For each experimental condition, we obtain an  $n_{\text{test}} \times B$  prediction matrix  $\hat{\mathbf{P}}$ , from which individual-level ePIW and eDFR are computed.

### 4.2 Results on Simulated Data

We first study individual-level prediction instability in a controlled synthetic setting where the data-generating process is known. Data are generated from a logistic regression model with five predictors, where three features carry signal and two represent noise. This design yields a balanced classification task with an estimated decision threshold near  $\tau \approx 0.53$  and represents a moderate signal-to-noise regime.

**Aggregate performance and competitiveness.** Table 2 shows how all model specifications considered are competitive under standard aggregate performance metrics, where differences in out-of-sample loss and accuracy across model classes are small, and variability across retraining runs for a given model architecture is negligible. From the perspective of conventional evaluation criteria, these models are therefore practically indistinguishable.

Table 2: Aggregate out-of-sample performance on simulated data (mean  $\pm$  1 SD across  $B = 100$  retrainings) evaluated on Binary Cross-entropy (BCE) and accuracy

Model	Resampled training data				Fixed training data			
	$n_{\text{train}} = 500$		$n_{\text{train}} = 5000$		$n_{\text{train}} = 500$		$n_{\text{train}} = 5000$	
	BCE	Acc.	BCE	Acc.	BCE	Acc.	BCE	Acc.
Log-LBFGS	0.523 $\pm$ .004	73.4% $\pm$ .4	0.518 $\pm$ .001	74.1% $\pm$ .1	0.517 $\pm$ .000	74.1% $\pm$ .0	0.519 $\pm$ .000	74.0% $\pm$ .0
Log-SGD	0.520 $\pm$ .003	73.8% $\pm$ .3	0.517 $\pm$ .001	74.1% $\pm$ .1	0.517 $\pm$ .000	74.0% $\pm$ .1	0.517 $\pm$ .000	74.0% $\pm$ .1
Log-poly	0.534 $\pm$ .006	72.4% $\pm$ .6	0.520 $\pm$ .001	74.1% $\pm$ .1	0.527 $\pm$ .001	73.2% $\pm$ .0	0.520 $\pm$ .001	74.0% $\pm$ .0
NN-1L	0.529 $\pm$ .004	73.6% $\pm$ .3	0.519 $\pm$ .001	74.1% $\pm$ .1	0.527 $\pm$ .001	73.7% $\pm$ .1	0.519 $\pm$ .001	74.3% $\pm$ .1
NN-2L	0.536 $\pm$ .006	73.0% $\pm$ .5	0.519 $\pm$ .001	74.1% $\pm$ .1	0.536 $\pm$ .002	73.3% $\pm$ .1	0.519 $\pm$ .000	74.0% $\pm$ .1

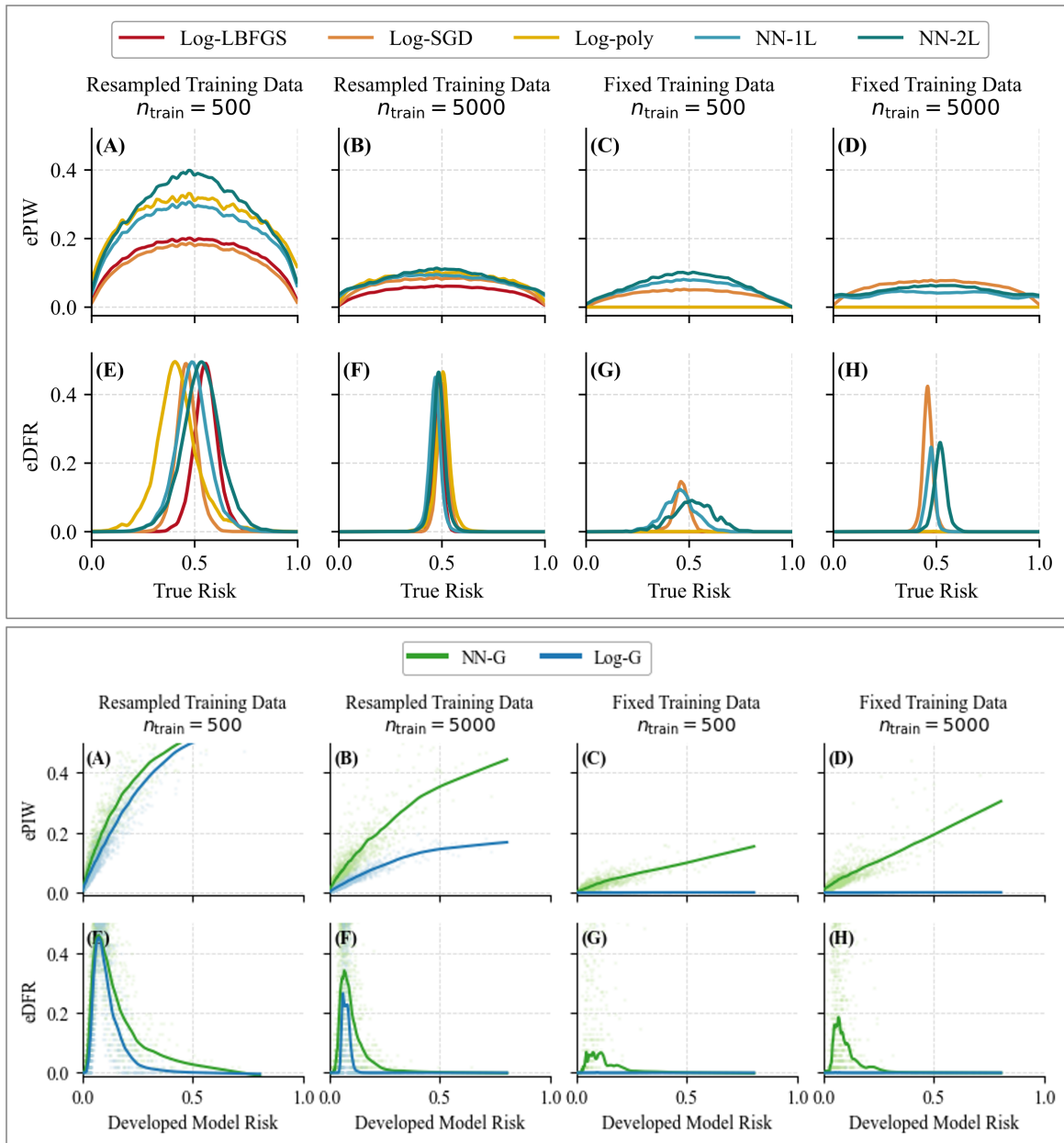


Figure 1: Individual-level prediction instability in simulation (top) and the GUSTO-I clinical dataset (bottom). Panels (A–D) report empirical prediction interval width (ePIW); panels (E–H) report empirical decision flip rate (eDFR). Columns correspond to resampled training data versus fixed training data (random-seed variation only), each evaluated at  $n_{\text{train}} \in \{500, 5000\}$ . In the simulated setting, instability is plotted as a function of true risk; in GUSTO-I, instability is plotted as a function of developed model risk. Across both settings, prediction dispersion is consistently larger for neural networks than for logistic regression and attenuates with increasing training sample size under resampled training data. Decision instability concentrates near clinical decision thresholds and diminishes with increased data and reduced sources of randomness.

**Individual-level prediction instability.** Figure 1 summarizes individual-level instability across the test population using the proposed metrics ePIW and eDFR. Model capacity and optimization procedures are influential in shaping instability in the prediction space. Based on the observed distributions, instability is concentrated among individuals with intermediate true risk, while predictions for low- and high-risk individuals are relatively more stable. Specifically, individuals whose risk lies near the clinical decision boundary ( $\tau = 0.53$ ) receive the least reliable predictions.

Increasing the training sample size to  $n_{train} = 5000$  reduces instability under resampled training data for all models, but does not eliminate it. Under fixed training data, models trained with stochastic optimization continue to exhibit meaningful instability, whereas deterministic optimization procedures yield stable individual predictions. Notably, for the highly flexible neural network models (NN-1L, NN-2L), instability induced by random seed variation alone is comparable in magnitude to that induced by resampling the training data. The eDFR curves show that under resampled training data, decision instability follows a similar qualitative pattern across model classes, with flip rates peaking near the decision threshold, whereas under fixed training data, nonzero eDFR arises almost exclusively from models trained with stochastic optimization. Again, for the high-capacity neural networks (NN-1L, NN-2L), randomness in the optimization procedure alone induces decision instability comparable in magnitude to that from resampling the training data. Binned summaries of ePIW and eDFR by true-risk strata for all experimental conditions are reported in Appendix A.

The prediction space can also be evaluated on an individual basis to illustrate the heterogeneity of these distributions. Figure 2 displays the empirical risk distributions ( $\hat{P}_i$ ) for 12 representative individuals, revealing that while all models achieve comparable aggregate performance, their individual-level risk assignments diverge significantly as model complexity increases. This behavior is further shown in Figure 3, which tracks the predictions for a single out-of-sample individual (true risk = 0.381) across 100 pipeline instantiations. Population-level summaries of prediction interval width, bias, and mean squared error are reported in Appendix A.

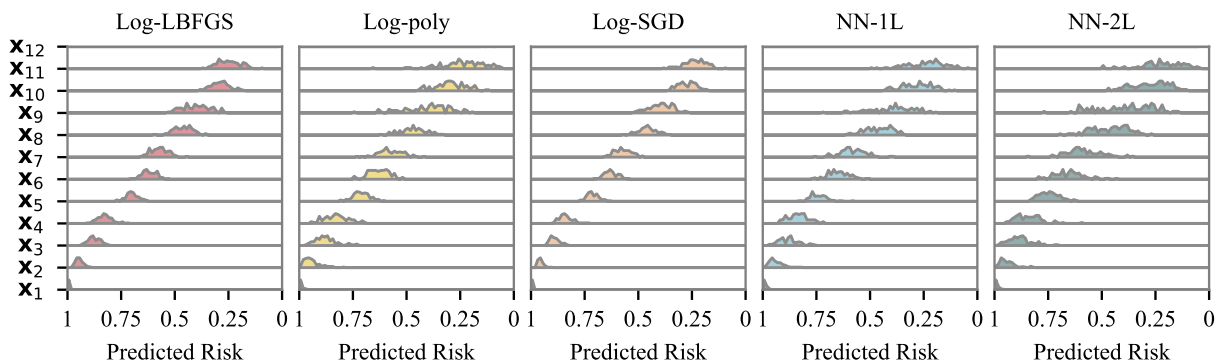


Figure 2: Individual-level prediction distributions across model families. Each panel displays the empirical distribution of predicted risks ( $\hat{P}_i$ ) for 12 representative individuals ( $x_1$  through  $x_{12}$ ) across  $B$  repeated instantiations of the learning pipeline from resampling the training data. From left to right, the panels represent: (1) Log-LBFGS, (2) Log-poly, (3) Log-SGD, (4) NN-1L, and (5) NN-2L. While all models satisfy the competitiveness criterion, the ridge plots reveal varying degrees of individual-level dispersion, particularly as model complexity evolves to neural network architectures.

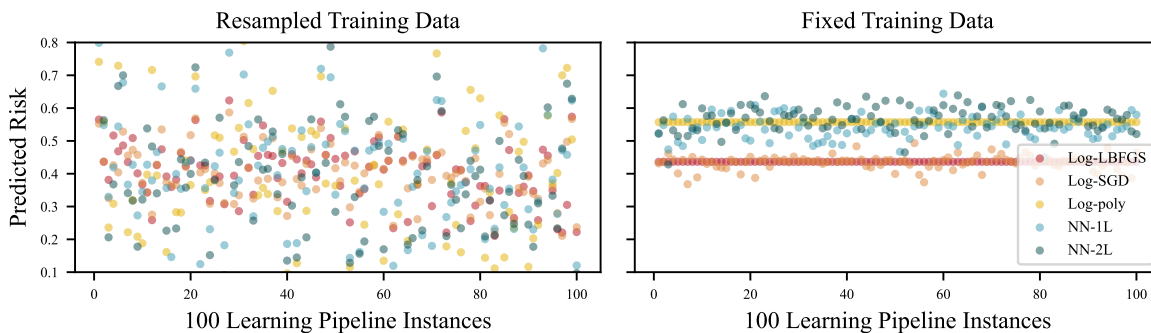


Figure 3: Prediction instability for a fixed out-of-sample individual (true risk = 0.381) under  $B = 100$  learning pipeline (LP) instances with  $n_{train} = 500$  from simulation data. Each point denotes the predicted risk from one fitted model instance. **Left:** variability induced by resampling the training data. **Right:** variability induced by random seed initialization with fixed training data.

**Implications.** The magnitude of instability observed in these experiments has serious consequences for the clinical utility and deployment of machine learning. As shown in the example provided in Figure 3, a high-capacity neural

network (NN-2L) can yield risk estimates that fluctuate across a critical treatment threshold based solely on the random initialization seed. For a clinician, this procedural arbitrariness implies that a patient’s eligibility for life-saving intervention or intensified monitoring could hinge on the randomness in the optimization path. For the ML practitioner, this stability gap reveals a hidden dimension of risk that remains invisible under standard aggregate validation protocols (e.g., population-level AUC or Brier scores). We find in certain cases that the instability induced by the random seed variability in learning pipeline can be as impactful as resampling the entire training dataset. Yet, these model conditions are rarely audited. Without explicitly diagnosing the sensitivity of individual predictions to the learning pipeline, we risk deploying models that satisfy static benchmarks but fail the fundamental requirement of individual-level clinical consistency.

### 4.3 Results on Clinical Risk Prediction (GUSTO-I)

We next assess individual-level prediction stability in a real clinical risk prediction task using the GUSTO-I trial on 30-day mortality following acute myocardial infarction [1]. The outcome prevalence is 7%, and the distribution of developed risk is highly skewed toward low values, with a clinically relevant decision threshold near  $\tau \approx 0.07$ .

As shown in Table 3, all model specifications remain competitive under standard aggregate performance metrics (e.g., AUC and Brier score) across both training sample sizes. However, Figure 1 reveals substantial disparities in individual-level stability that are obscured by population-level evaluation. Consistent with our simulation findings, neural network architectures exhibit markedly greater dispersion in predicted risk ( $\hat{P}_i$ ) compared to logistic regression models under all experimental conditions.

Table 3: Aggregate out-of-sample performance on GUSTO-I (mean  $\pm$  1 SD across  $B = 100$  retrainings).

Model	Resampled training data				Fixed training data			
	$n = 500$		$n = 5000$		$n = 500$		$n = 5000$	
	BCE	Acc.	BCE	Acc.	BCE	Acc.	BCE	Acc.
Log-G	0.22 $\pm$ .01	0.93 $\pm$ .00	0.21	0.93 $\pm$ .00	0.22	0.93 $\pm$ .00	0.21	0.93 $\pm$ .00
NN-G	0.22 $\pm$ .01	0.93 $\pm$ .01	0.22	0.93 $\pm$ .00	0.23	0.92 $\pm$ .01	0.21	0.93 $\pm$ .01

A critical distinction in the clinical setting is the localized nature of instability along the risk spectrum. While the simulation showed instability concentrated near the  $\tau \approx 0.53$  boundary, the GUSTO-I analysis demonstrates that significant prediction dispersion (ePIW) occurs in the upper tail of the distribution. Because the clinical threshold ( $\tau \approx 0.07$ ) is relatively low, much of this neural-network-induced variability occurs in regions that do not necessarily trigger a change in binary treatment assignments. For practitioners, this highlights a vital nuance, where elevated prediction instability does not strictly translate to decision instability (eDFR) if the dispersion is distal to the actionable threshold. Nevertheless, for high-risk patients, these fluctuations in mortality estimates can significantly undermine a clinician’s confidence in the model’s precision, even if the "high-risk" classification itself remains technically stable.

**Implications.** The GUSTO-I results demonstrate that prediction stability is a heterogeneous property varying across the risk manifold. The observed instability is a form of procedural epistemic uncertainty, wherein variance in the posterior risk estimates  $P(Y = 1|X)$  arises not from the underlying data-generating process, but from the stochasticity inherent in the learning pipeline  $\mathcal{A}$ . For observations near the decision boundary, this variance manifests as binary prediction instability, where the classification  $\hat{d}_i$  becomes critically sensitive to the local optima reached by the optimizer. Conversely, risk score instability occurring distal to the binary threshold poses a significant credibility risk, particularly in clinical applications where the specific risk probability is over-interpreted.

## 5 Discussion

Individual-level prediction instability is an often overlooked barrier to the deployment of machine learning in healthcare. It may not be immediately obvious why instability in individual-level predictions is problematic in practice. First, the variance of a risk estimate is often overlooked. Second, the only working optimization routine may also be contributing significantly to the instability. One might argue that variability across model fits is an inherent feature of predictive modeling, and that different models will naturally sort individuals differently. However, not only may the dependency of the predictions on the learning algorithm be a useful quality to know and communicate, but the sensitivity of individual predictions represents an additional and largely unexamined source of uncertainty that merits explicit consideration alongside standard measures of generalization performance. While statistical learning literature

has long recognized that flexible models can be more sensitive to arbitrary changes in the training data [20] and hence can exhibit overly optimistic training performance, our findings highlight a distinct, complementary concern. This concern being that flexible models can also be more sensitive to arbitrary changes to the learning pipeline. We do not claim that optimization-induced instability is equivalent to overfitting in the traditional sense; rather, it represents a form of procedural arbitrariness where a patient’s treatment eligibility is determined as much by the random initialization of the model as by their clinical data.

From a methodological perspective, our results expose the fragility of evaluating predictive models based on a single fitted instance. Relying on a single training run obscures meaningful variability; likewise, relying on a single risk estimate mistakes a stochastic snapshot for a definitive clinical truth. This is particularly problematic for overparameterized models where the loss landscape contains many nearly-equivalent local minima that nonetheless produce divergent clinical recommendations. In extreme cases, individual predictions may be effectively determined by random initialization rather than stable structure in the data. For certain modeling architectures and optimization procedures, a reported risk score is often better understood as a realization from a wide distribution of possible scores.

The evaluation framework we propose provides a practical way to characterize the sensitivity of the model to the learning pipeline (e.g., data, hyperparameters, computational settings). This framework can be especially valuable when comparing model families that are otherwise indistinguishable under conventional performance metrics. Our results advocate for a stability-aware interpretation of Occam’s razor: when out-of-sample performance is comparable, the more constrained model, such as a logistic regression model, can produce more reliable predictions compared to a neural network. By preferring models with greater individual-level stability, we mitigate the risk of procedural arbitrariness and ensure that clinical decisions are rooted in patient data rather than algorithmic noise. In high-stakes healthcare, where a "decision flip" can alter a patient’s care trajectory, individual-level instability should be elevated from a secondary consideration to a primary criterion for model selection.

Finally, these findings help contextualize the "uselessness" described by [4] and the persistent skepticism among clinical stakeholders. Skepticism toward AI is often dismissed as a lack of technical literacy [21] or resistance to change [22]. Our results suggest a more grounded justification: even when an overparameterized model appears accurate in aggregate, its individual-level predictions may be functionally inconsistent. From a clinician’s perspective, a model that flips its recommendation for the same patient across retrainings is not a reliable tool. Caution toward deployment, therefore, is not a rejection of innovation, but a rational response to a form of uncertainty that has been largely invisible under conventional validation practices. By making this variability explicit, our diagnostics provide a necessary bridge between technical validation and the rigorous reliability required for clinical care.

#### Box 1: Practitioner Checklist for Clinical Prediction Stability

To operationalize the assessment of individual-level reliability, we propose the following checklist for evaluating whether a model’s procedural consistency meets the standards required for high-stakes healthcare deployment:

- What is the dispersion of an individual’s risk score across repeated retrainings?
- How frequently do perturbations in the learning pipeline cause a patient’s classification to flip?
- Are there specific subpopulations or risk strata where prediction instability is disproportionately high?

## 5.1 Limitations

This work has several limitations. First, our proposed diagnostics require repeated model retraining, which may be computationally demanding for large-scale or resource-intensive models. Second, our analysis focuses on variability induced by resampling the training data and stochastic optimization procedures, and does not account for other sources of uncertainty such as label noise, distribution shift, or unmeasured confounding. Third, while we consider representative model classes spanning a range of expressive capacity, our findings may not generalize to all architectures or training regimes. Fourth, our stability metrics are empirical and descriptive; they do not provide formal uncertainty guarantees for individual predictions. Finally, our clinical evaluation is limited to a single risk prediction task and dataset, and broader validation across clinical domains and decision contexts is needed to assess the generality of these findings.

## 6 Conclusion

This work demonstrates that clinical prediction models with indistinguishable aggregate performance can nonetheless exhibit substantial, hidden variability at the level of individual predictions. We show that this instability arises not only from variations in training data but also from stochastic elements inherent to the learning pipeline, such as random

initialization and optimization noise. Our results indicate that for high-capacity models, these optimization-induced fluctuations can be as impactful as resampling the entire training dataset.

To make this phenomenon operational, we introduced two model-agnostic diagnostics: empirical prediction interval width (ePIW) and empirical decision flip rate (eDFR). Ultimately, we find that individual-level instability can be valuable to incorporate for overparameterized clinical model evaluations. By incorporating stability diagnostics into standard validation workflows, practitioners can move beyond aggregate metrics to ensure that model-assisted decisions are robust to the arbitrary elements of the machine learning pipeline. When multiple model specifications achieve comparable out-of-sample performance, our results suggest that a selection strategy centered on procedural consistency can be warranted: prioritizing more constrained models that yield stable individual-level predictions may be a necessary step toward building the trust and reliability required for high-stakes clinical deployment.

## References

- [1] The GUSTO Investigators. An international randomized trial comparing four thrombolytic strategies for acute myocardial infarction. *The New England Journal of Medicine*, 329(10):673–682, 1993.
- [2] John Atkinson and Emily Atkinson. Machine learning and healthcare: Potential benefits and issues. *The Journal of Ambulatory Care Management*, 46(2):114–120, 2023.
- [3] Eric Poon, Christopher Lemak, Jorge Rojas, Joseph Guptill, and David Classen. Adoption of artificial intelligence in healthcare: Survey of health system priorities, successes, and challenges. *Journal of the American Medical Informatics Association*, 32(7):1093–1100, 2025.
- [4] Florian Markowitz. All models are wrong and yours are useless: making clinical prediction models impactful for patients. *npj Precision Oncology*, 8(1):54, 2024.
- [5] Ewout W. Steyerberg, Marinus J. C. Eijkemans, Eric Boersma, J. Dik F. Habbema, and Hans C. van Houwelingen. Equally valid models gave divergent predictions for mortality in acute myocardial infarction patients in a comparison of logistic regression models. *Journal of Clinical Epidemiology*, 58(4):383–390, 2005.
- [6] Richard D. Riley, Danielle van der Windt, Peter Croft, and Karel G. M. Moons, editors. *Prognosis Research in Healthcare: Concepts, Methods and Impact*. Oxford University Press, Oxford, UK, 2019.
- [7] Leo Breiman. Statistical modeling: The two cultures. *Statistical Science*, 16(3):199–215, 2001.
- [8] Lesia Semenova, Cynthia Rudin, and Ronald E. Parr. On the existence of simpler machine learning models. In *Proceedings of the Conference on Fairness, Accountability, and Transparency (FAT\*)*, 2019.
- [9] Mikhail Belkin, Daniel Hsu, and Partha Mandal. Reconciling modern machine-learning practice and the classical bias–variance trade-off. *Proceedings of the National Academy of Sciences*, 116(32):15849–15854, 2019.
- [10] Trevor Hastie, Andrea Montanari, Saharon Rosset, and Ryan J. Tibshirani. Surprises in high-dimensional ridgeless least squares interpolation. *The Annals of Statistics*, 50(2):949–986, 2022.
- [11] Alexander D’Amour, Katherine Heller, Dan Moldovan, Ben Adlam, Babak Alipanahi, Alex Beutel, Christina Chen, Jonathan Deaton, Jacob Eisenstein, Matthew D. Hoffman, Soroosh Hormoz, Neil Houlsby, Jared Kaplan, Sam McCandlish, Michael McLaughlin, Vladimir Mikulik, Yaniv Ovadia, Adam Pearce, Shuang Song, Jacob Steinhardt, D. Sculley, Jasper Snoek, Sandeep Srinivasan, Alex Tamkin, Mingxing Tan, N. Vieillard, Yuxi Wang, Xinyang Wang, Ziyu Wang, Yi Wu, Qiaochu Xu, and Xiaohua Zhai. Underspecification presents challenges for credibility in modern machine learning. *Journal of Machine Learning Research*, 23:1–61, 2022.
- [12] Jonas Mehrer, Courtney J. Spoerer, Nikolaus Kriegeskorte, and Tim C. Kietzmann. Individual differences among deep neural network models. *Nature Communications*, 11, 2020.
- [13] Charles Marx, Flavio Calmon, and Berk Ustun. Predictive multiplicity in classification. In *Proceedings of the 37th International Conference on Machine Learning (ICML)*, 2020.
- [14] Richard D. Riley and Gary S. Collins. Stability of clinical prediction models developed using statistical or machine learning methods. *Biometrical Journal*, 65(8), 2023.
- [15] Hyeonwoo Noh, Taesup You, Jonghwan Mun, and Bohyung Han. Regularizing deep neural networks by noise: Its interpretation and optimization. In *Advances in Neural Information Processing Systems*, volume 30, 2017.
- [16] N. T. Bui, Guergana Savova, and Lijun Wang. Assessing the macro and micro effects of random seeds on fine-tuning large language models. In *Proceedings of the 14th International Joint Conference on Natural Language Processing and the 4th Conference of the Asia-Pacific Chapter of the Association for Computational Linguistics (IJCNLP-AAACL)*, Mumbai, India, 2025.

- [17] Pranav S. Madhyastha and J. Rishabh. On model stability as a function of random seed. In *Proceedings of the 23rd Conference on Computational Natural Language Learning (CoNLL)*, 2019.
- [18] Prakhar Ganesh, Usman Gohar, Lu Cheng, and Golnoosh Farnadi. Different horses for different courses: Comparing bias mitigation algorithms in ml. In *Workshop on Algorithmic Fairness through the Lens of Metrics and Evaluation (AFME) at NeurIPS*, 2024. arXiv:2411.11101.
- [19] Ian J. Goodfellow, Oriol Vinyals, and Andrew M. Saxe. Qualitatively characterizing neural network optimization problems. In *Proceedings of the International Conference on Learning Representations (ICLR)*, 2015. Published as a conference paper at ICLR 2015.
- [20] Bradley Efron. The estimation of prediction error: Covariance penalties and cross-validation. *Journal of the American Statistical Association*, 99(467):619–632, 2004.
- [21] [Initial] Kumar, [Initial] Singh, et al. Adoption challenges to artificial intelligence literacy in public healthcare: An evidence based study in saudi arabia. *Frontiers in Public Health*, 2025.
- [22] [Initial] Sobaih et al. Health care professionals’ concerns about medical ai and psychological barriers and strategies for successful implementation: Scoping review. *Journal of Medical Internet Research*, 27:e66986, 2025.

## A Supplementary Results and Figures

Table 4: Empirical prediction interval width (ePIW) by true-risk bin across training conditions.

True Risk (bin)	Log-LBFGS	Log-SGD	Log-poly	NN-1L	NN-2L
<b>Resampled training data, <math>n_{\text{train}} = 500</math></b>					
[0.0, 0.1)	0.104	0.089	0.230	0.184	0.205
[0.1, 0.2)	0.177	0.161	0.314	0.279	0.322
[0.2, 0.3)	0.223	0.205	0.369	0.342	0.411
[0.3, 0.4)	0.250	0.232	0.398	0.375	0.469
[0.4, 0.5)	0.260	0.240	0.407	0.389	0.491
[0.5, 0.6)	0.259	0.238	0.414	0.388	0.490
[0.6, 0.7)	0.245	0.220	0.390	0.358	0.449
[0.7, 0.8)	0.224	0.194	0.362	0.323	0.391
[0.8, 0.9)	0.184	0.152	0.324	0.275	0.323
[0.9, 1.0]	0.112	0.086	0.263	0.197	0.229
<b>Resampled training data, <math>n_{\text{train}} = 5000</math></b>					
[0.0, 0.1)	0.033	0.048	0.073	0.073	0.076
[0.1, 0.2)	0.056	0.082	0.104	0.096	0.101
[0.2, 0.3)	0.070	0.102	0.120	0.121	0.126
[0.3, 0.4)	0.078	0.111	0.129	0.130	0.145
[0.4, 0.5)	0.081	0.114	0.130	0.128	0.154
[0.5, 0.6)	0.081	0.116	0.131	0.124	0.154
[0.6, 0.7)	0.077	0.111	0.125	0.116	0.138
[0.7, 0.8)	0.070	0.101	0.116	0.105	0.118
[0.8, 0.9)	0.058	0.082	0.099	0.088	0.096
[0.9, 1.0]	0.034	0.047	0.066	0.074	0.078
<b>Fixed training data, <math>n_{\text{train}} = 500</math></b>					
[0.0, 0.1)	0.000	0.034	0.000	0.038	0.036
[0.1, 0.2)	0.000	0.059	0.000	0.064	0.066
[0.2, 0.3)	0.000	0.073	0.000	0.085	0.099
[0.3, 0.4)	0.000	0.080	0.000	0.102	0.124
[0.4, 0.5)	0.000	0.083	0.000	0.107	0.137
[0.5, 0.6)	0.000	0.084	0.000	0.107	0.136
[0.6, 0.7)	0.000	0.079	0.000	0.101	0.121
[0.7, 0.8)	0.000	0.072	0.000	0.088	0.093
[0.8, 0.9)	0.000	0.061	0.000	0.063	0.057
[0.9, 1.0]	0.000	0.035	0.000	0.028	0.022
<b>Fixed training data, <math>n_{\text{train}} = 5000</math></b>					
[0.0, 0.1)	0.000	0.040	0.000	0.046	0.049
[0.1, 0.2)	0.000	0.070	0.000	0.052	0.059
[0.2, 0.3)	0.000	0.090	0.000	0.066	0.077
[0.3, 0.4)	0.000	0.101	0.000	0.073	0.087
[0.4, 0.5)	0.000	0.105	0.000	0.069	0.093
[0.5, 0.6)	0.000	0.107	0.000	0.069	0.095
[0.6, 0.7)	0.000	0.099	0.000	0.072	0.088
[0.7, 0.8)	0.000	0.089	0.000	0.068	0.073
[0.8, 0.9)	0.000	0.072	0.000	0.055	0.057
[0.9, 1.0]	0.000	0.042	0.000	0.046	0.051

Table 5: Empirical decision flip rate (eDFR) by true-risk bin across training conditions.

True Risk (bin)	Log-LBFGS	Log-SGD	Log-poly	NN-1L	NN-2L
<b>Resampled training data, <math>n_{\text{train}} = 500</math></b>					
[0.0, 0.1)	0.000	0.000	0.001	0.000	0.000
[0.1, 0.2)	0.000	0.000	0.007	0.001	0.002
[0.2, 0.3)	0.000	0.000	0.027	0.010	0.022
[0.3, 0.4)	0.026	0.015	0.115	0.082	0.127
[0.4, 0.5)	0.304	0.275	0.390	0.369	0.398
[0.5, 0.6)	0.313	0.285	0.381	0.361	0.404
[0.6, 0.7)	0.031	0.016	0.112	0.076	0.121
[0.7, 0.8)	0.001	0.000	0.032	0.011	0.023
[0.8, 0.9)	0.000	0.000	0.009	0.001	0.003
[0.9, 1.0]	0.000	0.000	0.003	0.000	0.000
<b>Resampled training data, <math>n_{\text{train}} = 5000</math></b>					
[0.0, 0.1)	0.000	0.000	0.000	0.000	0.000
[0.1, 0.2)	0.000	0.000	0.000	0.000	0.000
[0.2, 0.3)	0.000	0.000	0.000	0.000	0.000
[0.3, 0.4)	0.000	0.000	0.005	0.001	0.001
[0.4, 0.5)	0.104	0.130	0.168	0.140	0.155
[0.5, 0.6)	0.116	0.142	0.183	0.149	0.173
[0.6, 0.7)	0.000	0.000	0.003	0.000	0.001
[0.7, 0.8)	0.000	0.000	0.000	0.000	0.000
[0.8, 0.9)	0.000	0.000	0.000	0.000	0.000
[0.9, 1.0]	0.000	0.000	0.000	0.000	0.000
<b>Fixed training data, <math>n_{\text{train}} = 500</math></b>					
[0.0, 0.1)	0.000	0.000	0.000	0.000	0.000
[0.1, 0.2)	0.000	0.000	0.000	0.000	0.000
[0.2, 0.3)	0.000	0.000	0.000	0.002	0.004
[0.3, 0.4)	0.000	0.000	0.000	0.017	0.022
[0.4, 0.5)	0.000	0.059	0.000	0.076	0.062
[0.5, 0.6)	0.000	0.062	0.000	0.099	0.083
[0.6, 0.7)	0.000	0.000	0.000	0.022	0.038
[0.7, 0.8)	0.000	0.000	0.000	0.002	0.007
[0.8, 0.9)	0.000	0.000	0.000	0.000	0.000
[0.9, 1.0]	0.000	0.000	0.000	0.000	0.000
<b>Fixed training data, <math>n_{\text{train}} = 5000</math></b>					
[0.0, 0.1)	0.000	0.000	0.000	0.000	0.000
[0.1, 0.2)	0.000	0.000	0.000	0.000	0.000
[0.2, 0.3)	0.000	0.000	0.000	0.000	0.000
[0.3, 0.4)	0.000	0.000	0.000	0.000	0.000
[0.4, 0.5)	0.000	0.101	0.000	0.050	0.069
[0.5, 0.6)	0.000	0.134	0.000	0.079	0.111
[0.6, 0.7)	0.000	0.000	0.000	0.000	0.001
[0.7, 0.8)	0.000	0.000	0.000	0.000	0.000
[0.8, 0.9)	0.000	0.000	0.000	0.000	0.000
[0.9, 1.0]	0.000	0.000	0.000	0.000	0.000

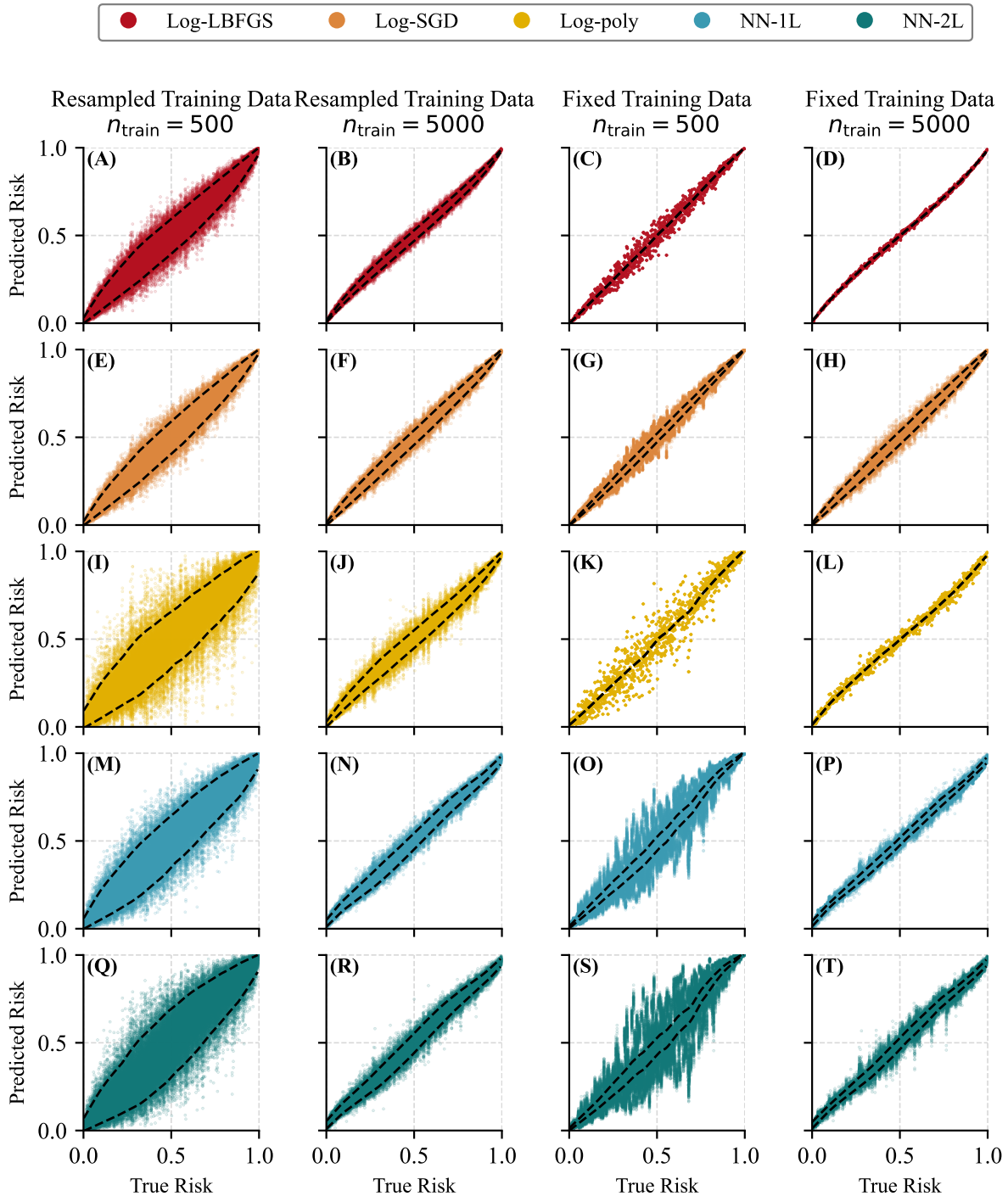


Figure 4: Predicted risk versus true risk across model classes, training sample sizes, and sources of stochasticity. Each row corresponds to a model specification (Log-LBFGS, Log-SGD, Log-poly, NN-1L, NN-2L). Columns report results under resampled training data and fixed training data (random-seed variation only), each evaluated at  $n_{\text{train}} \in \{500, 5000\}$ . Points represent individual-level predicted risks evaluated on a common test set across  $B = 100$  model retrains. The dashed 45° line indicates perfect calibration ( $\hat{p} = p_{\text{true}}$ ).

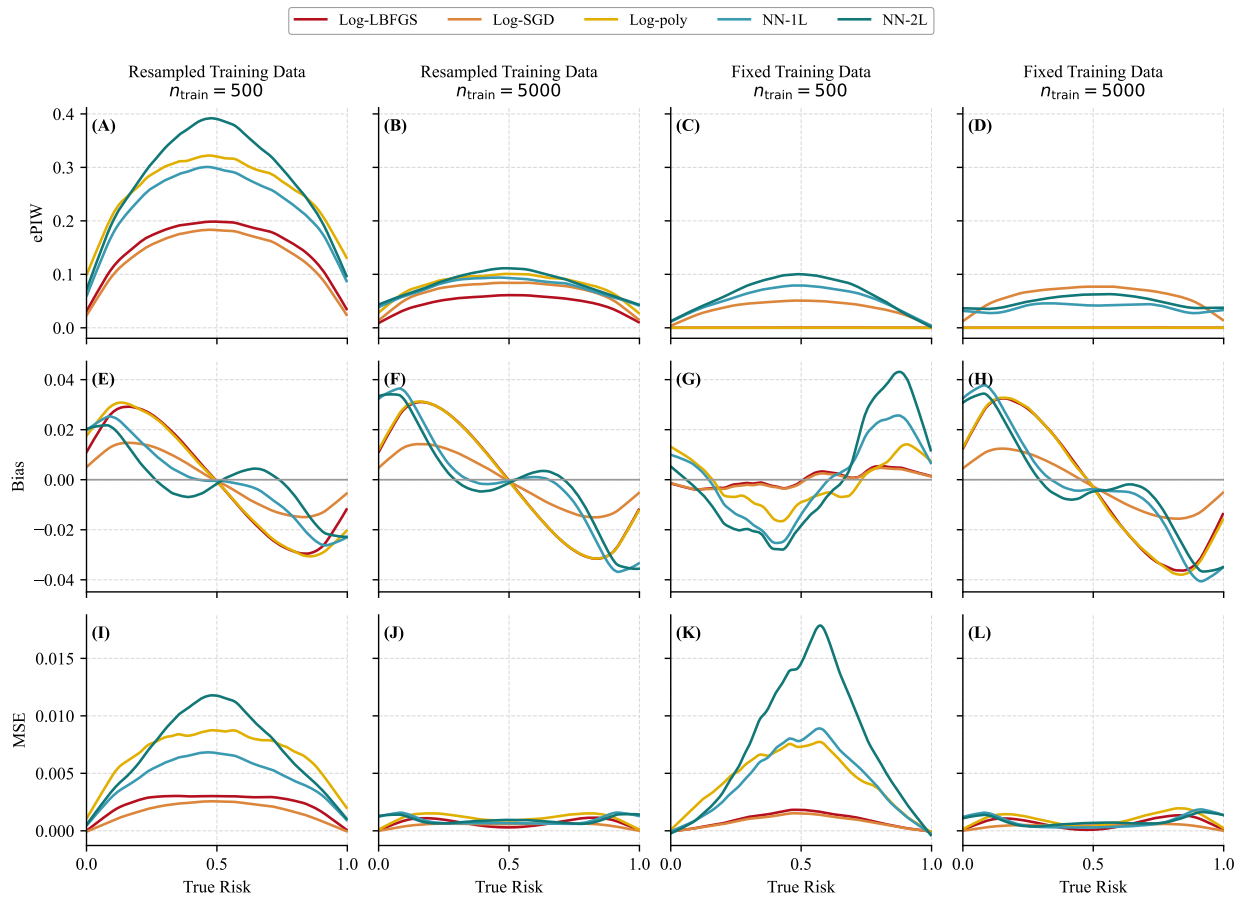


Figure 5: Individual-level prediction instability, bias, and mean squared error as functions of true risk in the simulated setting. Columns correspond to resampled training data and fixed training data, each evaluated at  $n_{\text{train}} \in \{500, 5000\}$ . Rows report empirical prediction interval width (ePIW; top), prediction bias (middle), and mean squared error (MSE; bottom), with LOESS smoothing applied to highlight systematic trends across the true-risk spectrum. Curves correspond to different model classes.